Loss of class I_A PI3K signaling in muscle leads to impaired muscle growth, insulin response, and hyperlipidemia

Ji Luo,[1] Cassandra L. Sobkiw,[1] Michael F. Hirshman,[2] M. Nicole Logsdon,[1] Timothy Q. Li,[1] Laurie J. Goodyear,[2] and Lewis C. Cantley[1,*]

[1] Department of Systems Biology, Harvard Medical School, and Division of Signal Transduction, Beth Israel Deaconess Medical Center, Boston, Massachusetts 02115
[2] Research Division, Joslin Diabetes Center, and Department of Medicine, Brigham and Women's Hospital and Harvard Medical School, Boston, Massachusetts 02215
*Correspondence: lewis_cantley@hms.harvard.edu

Summary

The evolutionarily conserved phosphoinositide 3-kinase (PI3K) signaling pathway mediates both the metabolic effects of insulin and the growth-promoting effects of insulin-like growth factor-1 (IGF-1). We have generated mice deficient in both the p85α/p55α/p50α and the p85β regulatory subunits of class I_A PI3K in skeletal muscles. PI3K signaling in the muscle of these animals is severely impaired, leading to a significant reduction in muscle weight and fiber size. These mice also exhibit muscle insulin resistance and whole-body glucose intolerance. Despite their ability to maintain normal fasting and fed blood glucose levels, these mice show increased body fat content and elevated serum free fatty acid and triglyceride levels. These results demonstrate that in vivo p85 is a critical mediator of class I_A PI3K signaling in the regulation of muscle growth and metabolism. Our finding also indicates that compromised muscle PI3K signaling could contribute to symptoms of hyperlipidemia associated with human type 2 diabetes.

Introduction

Class I_A phosphoinositide 3-kinases (PI3Ks) are a family of lipid kinases that phosphorylates the 3′-OH position on the inositol ring of phosphatidylinositol-4,5-bisphosphate (PIP_2) to generate the lipid second messenger phosphatidylinositol-3,4,5-trisphosphate (PIP_3) (Cantley, 2002). In mammalian cells class I_A PI3Ks regulate cell metabolism and cell growth downstream of the insulin and the insulin-like growth factor-1 (IGF-1) receptors, respectively (LeRoith et al., 1995; Saltiel and Kahn, 2001). Activation of these receptors leads to tyrosine phosphorylation of the insulin receptor substrate (IRS) family of adaptor molecules, particularly IRS-1 and IRS-2. IRS proteins in turn recruit and activate class I_A PI3K (Virkamaki et al., 1999). The lipid phosphatase PTEN dephosphorylates the 3′ position on PIP_3 to regenerate PIP_2 and therefore terminates PI3K signaling (Cantley, 2002). This insulin-PI3K signaling pathway is highly conserved throughout evolution and critically regulates of growth and metabolism in *C. elegans* and *D. melanogaster* (Guarente and Kenyon, 2000).

Class I_A PI3K is a heterodimer consisting of a p85 regulatory subunit and a p110 catalytic subunit. The p85 regulatory subunit is essential for the stability of the p110 catalytic subunit (Yu et al., 1998b; Brachmann et al., 2005). In addition, p85 also mediates the activation and membrane recruitment of the p85-p110 heterodimer through the binding of its two Src-homology 2 (SH2) domains to phosphotyrosine residues on activated growth factor receptors or their adaptor molecules such as IRS-1 and IRS-2 (Yu et al., 1998a). In mammals, there exist multiple isoforms of p85 and p110. The major p85 isoforms p85α, p55α, and p50α are encoded by a single gene *pik3r1* through alternative transcription initiation sites. Two other minor isoforms, p85β and p55γ, are encoded by the genes *pik3r2* and *pik3r3,* respectively. The p85α/p55α/p50α and p85β isoforms are expressed ubiquitously whereas p55γ is enriched in the brain and the testis. Three genes, *pik3ca*, *pik3cb*, and *pik3cd*, encode the three class I_A PI3K catalytic subunit isoforms, p110α, p110β, and p110δ, respectively (Fruman et al., 1998).

A major downstream effector of PI3K signaling is the protein serine/threonine kinase Akt (also known as protein kinase B or PKB). Upon membrane recruitment by PIP_3, Akt becomes activated through phosphorylation at Thr-308 in its catalytic loop by the kinase PDK1 (Mora et al., 2004). Additional phosphorylation at Ser-473 of Akt leads to its full activation (Bayascas and Alessi, 2005). Akt regulates cell growth and metabolism through the phosphorylation of a number of target molecules. Akt phosphorylates and inactivates tuberin (TSC2), a component of the TSC1/TSC2 tuberous sclerosis protein complex. This relieves the inhibitory effect the TSC1/TSC2 complex exerts on the mammalian target of rapamycin (mTOR), thus allowing mTOR to promote protein synthesis and cell growth (Richardson et al., 2004). Akt also phosphorylates and inactivates the forkhead (FOXO) family of transcription factors that regulate the expression of a wide range of metabolic, survival and cell cycle genes (Barthel et al., 2005; Burgering and Medema, 2003). In insulin responsive tissues such as muscle and fat, Akt promotes the membrane translocation of the glucose transporter GLUT4 and thus increase cellular glucose uptake (Thong et al., 2005; Virkamaki et al., 1999). In addition, Akt promotes glycogen synthesis by phosphorylating and thus inactivating glycogen synthase kinase 3 (GSK3), an inhibitory kinase for glycogen synthase (Cohen and Frame, 2001).

Muscle atrophy is often associated with diseased states such as diabetes and cancer. In vitro studies have implicated the

IGF-1/PI3K signaling pathway in the regulation of myocyte growth (Rommel et al., 2001). Consistent with this, hyperactivation of Akt leads to muscle hypertrophy in vivo (Lai et al., 2004). At the molecular level, myocyte growth is thought to be promoted by Akt signaling through mTOR and GSK3 (Bodine et al., 2001; Rommel et al., 2001). In addition, Akt protects against muscle atrophy through its phosphorylation of the forkhead transcription factors. This inhibits forkhead-mediated transcription of atrogin-1 (also known as MAFbx) and MuRF1, two E3 ubiquitin ligases that promote muscle protein degradation (Sandri et al., 2004; Stitt et al., 2004).

Muscle insulin resistance has been implicated as a major contributor toward human type 2 diabetes (Shulman, 2004). Deletion of the insulin receptor in the muscle leads to muscle insulin resistance (Bruning et al., 1998), whereas deletion of PTEN in the muscle enhances insulin sensitivity and protects against diet-induced hyperglycemia (Wijesekara et al., 2005). PI3K/Akt signaling downstream of the insulin receptor has been implicated as a critical mediator of glucose uptake and glycogen synthesis in the muscle (Saltiel and Kahn, 2001).

Previously, we and others have generated mice lacking various class I_A PI3K subunits in order to understand their in vivo roles in growth and metabolism. Germline deletion of the *pik3r1* gene (i.e., deletion of all three isoforms p85α, p55α, and p50α) results in perinatal lethality, although surviving mice surprisingly show improved insulin sensitivity (Fruman et al., 2000). Similarly, mice heterozygous for the *pik3r1* gene, or mice lacking either p85α alone, p55α and p50α alone, or p85β all display improved PI3K signaling downstream of the insulin receptor (Chen et al., 2004; Terauchi et al., 1999; Ueki et al., 2002b; Mauvais-Jarvis et al., 2002). Subsequent studies revealed that under normal circumstances p85 is stoichiometrically in excess of p110 and monomeric p85 can inhibit PI3K signaling by sequestering tyrosine phosphorylated IRS-1 (Ueki et al., 2002a; Luo et al., 2005a). A partial reduction in total p85 levels therefore increases the ratio of p85-p110 heterodimer to p85 monomer, despite the overall reduction in total class I_A PI3K activity. This in turn allows improved PI3K signaling downstream of the insulin receptor. On the other hand, mouse embryonic fibroblasts (MEFs) lacking both *pik3r1* and *pik3r2* genes exhibit severely attenuated class I_A PI3K signaling, though the early lethality of *pik3r1*$^{-/-}$*pik3r2*$^{-/-}$ mice during embryogenesis precludes the analysis of p85 function in adult tissues (Brachmann et al., 2005).

To better understand the in vivo roles of the p85 regulatory subunit and to circumvent the lethality phenotype associated with the *pik3r1*$^{-/-}$ and the *pik3r1*$^{-/-}$*pik3r2*$^{-/-}$ germline knockout (KO) mice, we have engineered mice in which the *pik3r1* gene can be deleted in a tissue-specific fashion by the Cre-lox approach (Luo et al., 2005b). By crossing these mice onto the *pik3r2*$^{-/-}$ background, we were able to generate mice with p85α, p55α, p50α, and p85β all deleted in the tissue of interest. Here, we show that mice lacking both *pik3r1* and *pik3r2* in skeletal muscles (hereafter referred to as *pik3r1 mKO pik3r2*$^{-/-}$ mice) exhibit severely impaired PI3K signaling in skeletal muscles, thus demonstrating genetically that the p85 regulatory subunit is essential in mediating the activation of class I_A PI3K. These animals have smaller muscles that are associated with reduced fiber size. In addition, their skeletal muscles are insulin-resistant and consequently these mice are glucose intolerant. Fasting and fed glucose and insulin levels remain normal, however, suggesting adequate compensation from other insulin-sensitive tissues. Interestingly, these animals show increased adiposity and exhibit symptoms of hyperlipidemia that is associated with human type 2 diabetes. These results demonstrate that in vivo class I_A PI3K is both an important regulator of muscle growth and a critical mediator of insulin signaling in the muscle.

Results

Impaired muscle PI3K signaling in *pik3r1 mKO pik3r2*$^{-/-}$ mice

We engineered a conditional allele of the mouse *pik3r1* gene (*pik3r1*^{fl}) by flanking exon 7 with loxP sites. Cre-mediated deletion of exon 7 introduces a stop codon in the mRNA, thus ablating the expression of p85α, p55α and p50α proteins (Luo et al., 2005b). We crossed *pik3r1*$^{fl/fl}$ mice with *mck-cre* transgenic mice that express the Cre recombinase specifically in striated myocytes (Bruning et al., 1998) and obtained mice with muscle-specific deletion of the *pik3r1* gene (hereafter referred to as *pik3r1 mKO*). In the skeletal muscles of *pik3r1 mKO* mice we observed efficient deletion of p85α, p55α and p50α expression that is accompanied by a significant reduction in the levels of p110α protein (Figure 1A). We further crossed *pik3r1 mKO* mice with *pik3r2*$^{-/-}$ mice to generate *pik3r1 mKO pik3r2*$^{-/-}$ mice that lacked p85α, p55α, p50α and p85β proteins in the muscle (Figure 1C). The residual p85 proteins in the *pik3r1 mKO pik3r2*$^{-/-}$ mice might be attributed to other cell types in the muscle (such as satellite cells, adipocytes and endothelial cells) or the incomplete deletion of the *pik3r1* gene in a small fraction of myocytes.

The *mck-cre* transgene expresses in both the skeletal muscle and the heart. Previously we have characterized the cardiac phenotype of the *pik3r1 mKO pik3r2*$^{-/-}$ mice and demonstrated that these animals show reduced heart size and impaired cardiac hypertrophy (Luo et al., 2005b). In the present study, we focused on the skeletal muscle phenotype of these animals.

We first investigated PI3K signaling in skeletal muscles of these animals. Deletion of *pik3r1* alone or in combination with *pik3r2* resulted in a severe impairment of PI3K activation downstream of the insulin receptor. In both *pik3r1 mKO* and *pik3r1 mKO pik3r2*$^{-/-}$ mice, muscle IRS-1 and IRS-2 associated PI3K activities following insulin stimulation were reduced approximately 7- and 3- fold, respectively (Figure 1B). Interestingly, Akt activation, as judged by phosphorylation at Thr-308 and Ser-473, was only significantly attenuated in the muscles of *pik3r1 mKO pik3r2*$^{-/-}$ mice, but not in that of the *pik3r1 mKO* mice (Figure 1C). Previous studies using germline KO mice lacking Akt1 or Akt2 indicate that Akt1 predominately regulates growth whereas Akt2 predominately regulates glucose homeostasis (Cho et al., 2001a, 2001b; Tschopp et al., 2005). We therefore examined the activation of Akt1 and Akt2 separately by immunoprecipitation using isoform-specific antibodies. As shown in Figure 1C, similar to total Akt phosphorylation, we observed severe attenuation inT308 and S473 phosphorylation of both Akt1 and Akt2 in the muscle of *pik3r1 mKO pik3r2*$^{-/-}$ mice in response to insulin. Thus in vivo class I_A PI3K mediates the activation of both Akt1 and Akt2 by insulin in the muscle. Downstream of Akt, we found that insulin-stimulated phosphorylation of GSK3α/β and tuberin by Akt were significantly impaired in muscles of *pik3r1 mKO*

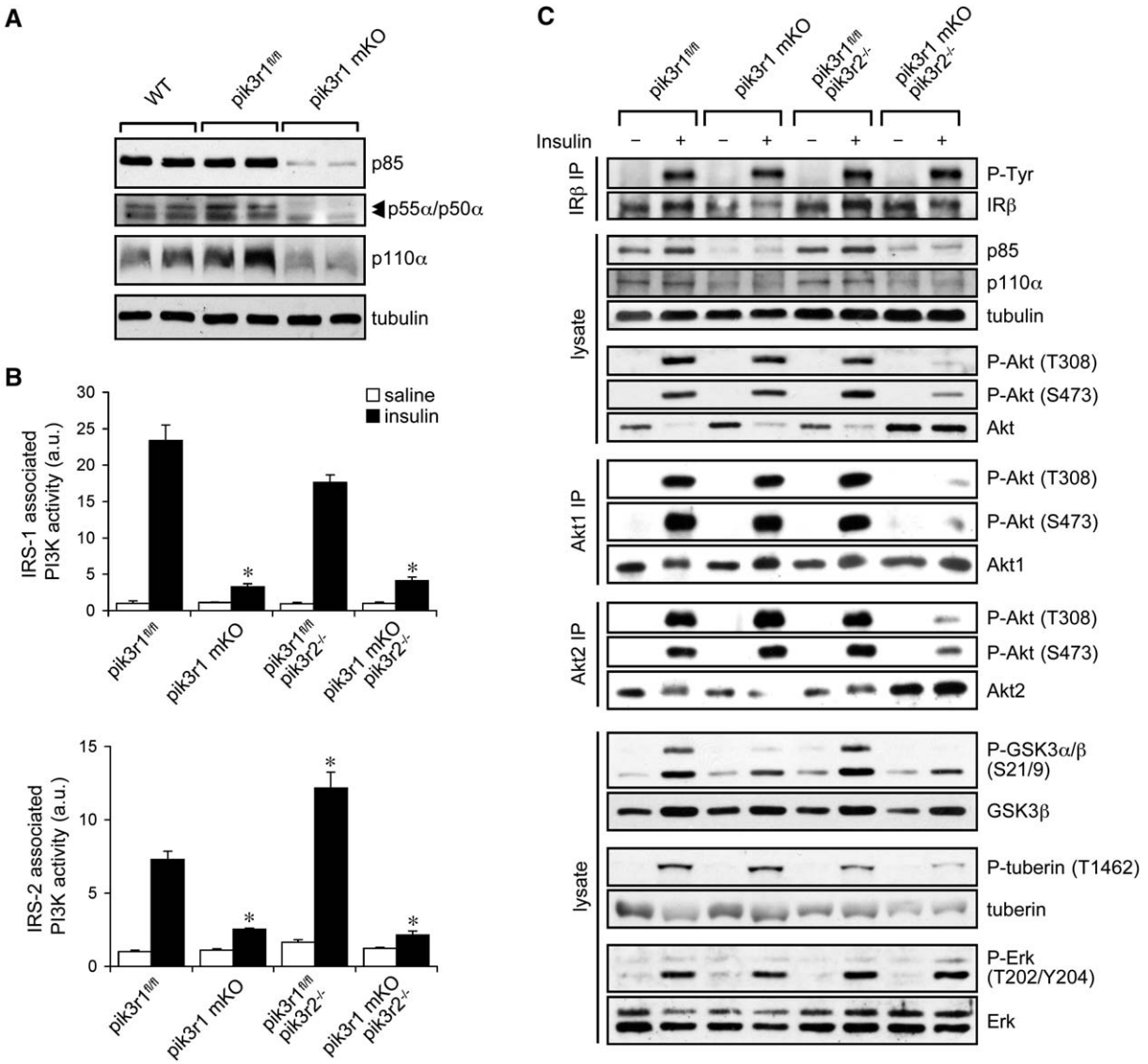

Figure 1. *pik3r1 mKO pik3r2*$^{-/-}$ mice show severely impaired PI3K signaling in skeletal muscles in response to insulin stimulation

A) Gastrocnemius muscle lysates from mice of the indicated genotypes were probed with anti-p85 and anti-p110α antibodies to assess the deletion efficiency of p85.
B) Mice were stimulated with either saline or 5 U/kg insulin for 5 min and PI3K activities associated with IRS-1 (top) and IRS-2 (bottom) immunoprecipitates from muscle lysates were measured by in vitro PI3K assay (n = 3, *p < 0.01 compared to *pik3r1*$^{fl/fl}$ mice of the same treatment group).
C) Mice were stimulated with either saline or 5 U/kg insulin for 5 min, Akt activation and Akt-mediated phosphorylation of downstream substrates in the muscle were assessed by Western blot using the appropriate phosphospecific antibodies (the total Akt antibody recognizes the unphosphorylated form of Akt better). Representative blots of 3 independent experiments are shown. All error bars represent standard errors of the mean.

pik3r2$^{-/-}$ mice (Figure 1C). GSK3α/β phosphorylation was also somewhat decreased in the muscle of some *pik3r1* mKO mice, although this result was variable. Otherwise, deletion of *pik3r1* alone or *pik3r2* alone had little effect on signaling downstream of Akt. As a control, Erk activation by insulin was unaffected in all cases. Taken together, these results suggest that in the absence of p85α isoforms, muscle PI3K signaling is severely compromised though Akt activation is largely unaffected. This could be due to compensation from the p85β isoform. When both p85α and p85β isoforms are ablated, however, muscle Akt signaling is severely impaired.

Muscle PI3K signaling downstream of the IGF-1 receptor has been implicated in the regulation of myocyte growth (Bodine et al., 2001; Rommel et al., 2001). We therefore investigated whether Akt activation downstream of IGF-1 receptor is also impaired in the muscle of *pik3r1 mKO pik3r2*$^{-/-}$ mice. Similar to that observed with insulin stimulation, IGF-1 mediated PI3K activation is also severely impaired in the muscle of these animals (Figure 2A). Again both Akt1 and Akt2 activation was significantly attenuated, resulting in reduced phosphorylation of downstream targets such as tuberin and GSK3 (Figure 2B).

Reduced muscle weight and myocyte size in *pik3r1 mKO pik3r2*$^{-/-}$ mice

As PI3K signaling has been implicated in the regulation of muscle growth and fiber size (Rommel et al., 2001), we investigated whether the *pik3r1 mKO pik3r2*$^{-/-}$ mice showed symptoms of muscle atrophy due to impaired PI3K signaling. Both male and

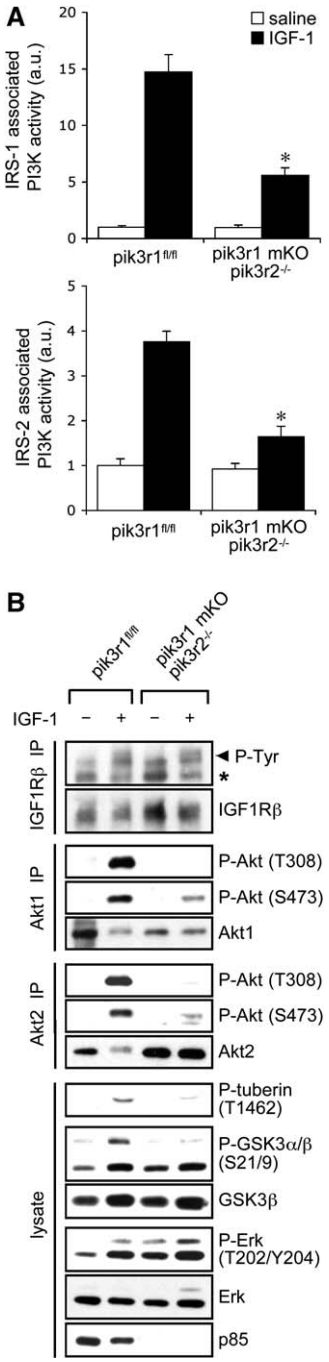

Figure 2. *pik3r1 mKO pik3r2*$^{-/-}$ mice show severely impaired PI3K signaling in skeletal muscles in response to IGF-1 stimulation

A) Control *pik3r1*$^{fl/fl}$ and *pik3r1 mKO pik3r2*$^{-/-}$ mice were stimulated with either saline or 1mg/kg IGF-1 for 7 min, and PI3K activities associated with IRS-1 (top) and IRS-2 (bottom) immunoprecipitates from muscle lysates were measured by in vitro PI3K assay (n = 3, *p < 0.01 compared to *pik3r1*$^{fl/fl}$ mice of the same treatment group).

B) Mice were stimulated with either saline or 1mg/kg IGF-1 for 7 min, Akt activation and Akt-mediated phosphorylation of downstream substrates in the muscle were assessed by Western blot using the appropriate phosphospecific antibodies (*cross-reacting band). Representative blots of 3 independent experiments are shown. All error bars represent standard errors of the mean.

female *pik3r1 mKO pik3r2*$^{-/-}$ mice have normal body weight (Figure 3A). Although in some study groups we observed a reduction in total body weight in some *pik3r1 mKO pik3r2*$^{-/-}$ mice, the difference did not reach overall statistical significance. The gastrocnemius muscles of the *pik3r1 mKO pik3r2*$^{-/-}$ mice, however, were approximately 30% lighter than control mice when normalized to body weight (Figure 3B). Thus loss of class I_A PI3K signaling in the muscle leads to a reduction in muscle weight. We next examined muscles fibers from *pik3r1 mKO pik3r2*$^{-/-}$ mice. Although histologically these fibers showed normal structure, they appeared to have smaller cross-sectional areas (Figure 3C). Indeed, morphormetric analysis of the tibialis anterior muscle from *pik3r1 mKO pik3r2*$^{-/-}$ mice revealed an approximately 40% reduction in both median and mean fiber size compared to age-matched mice of similar body weight (Figures 3D and 3E). Thus the reduction in muscle size in *pik3r1 mKO pik3r2*$^{-/-}$ mice can be attributed to a reduction in fiber size. Given that Akt mediated tuberin phosphorylation was attenuated in the muscle of *pik3r1 mKO pik3r2*$^{-/-}$ mice (Figures 1C and 2B), it is likely that impaired mTOR signaling and protein synthesis is at least in part responsible for the attenuated muscle growth in these animals. Consistent with this, we observed that in response to feeding, the muscle of *pik3r1 mKO pik3r2*$^{-/-}$ mice show attenuated Akt activation as well as phosphorylation of ribosomal S6 and 4EBP1, two key downstream effectors of mTOR that controls translation (Figure 3F).

Myocyte size can also be regulated by protein degradation. Fasting induces the expression of muscle E3-ubiquitin ligase atrogin-1/MAFbx and MuRF1 in a forkhead-dependent fashion. This facilitates muscle protein breakdown (Sandri et al., 2004; Stitt et al., 2004). We investigated whether atrogin-1/MAFbx and MuRF1 message levels were mis-regulated in *pik3r1 mKO pik3r2*$^{-/-}$ mice. Under the fed state, muscle atrogin-1/MAFbx and MuRF-1 mRNAs were below detection limit by real-time PCR for both control and *pik3r1 mKO pik3r2*$^{-/-}$ animals. During prolonged fasting, however, these mRNAs were markedly upregulated in animals of both genotypes. Unexpectedly, we found that muscle atrogin-1/MAFbx and MuRF1 mRNA levels were significantly lower in *pik3r1 mKO pik3r2*$^{-/-}$ mice compared to that of control mice (Figure 3G). Thus it is unlikely that the decreased muscle size is due to enhanced muscle atrophy in the *pik3r1 mKO pik3r2*$^{-/-}$ mice.

The small muscle size in *pik3r1 mKO pik3r2*$^{-/-}$ mice did not appear to significantly impair the animal's ability to perform chronic exercise. Using citrate synthase (CS) activity as an indicator of the muscle's response to exercise load, we found that under sedentary conditions muscle CS activity was only mildly reduced in the *pik3r1 mKO pik3r2*$^{-/-}$ mice. When subjected to aerobic exercise training for 1 month in the form of swimming, the increase in CS activity in *pik3r1 mKO pik3r2*$^{-/-}$ mice (149%) was comparable to that in WT mice (145%) (Figure 3H; Luo et al., 2005b).

pik3r1 mKO pik3r2$^{-/-}$ mice exhibit muscle insulin resistance, glucose intolerance, hyperlipidemia and increased adiposity

Skeletal muscle is a major insulin responsive tissue and a major site of glucose disposal in vivo. Muscle insulin resistance is a significant contributing factor toward human type 2 diabetes (Shulman, 2004). We first investigated insulin-stimulated glucose uptake in isolated soleus muscle (an oxidative muscle that is insulin responsive) and extensor digitorum longus (EDL) muscle (a glycolytic muscle that is less insulin responsive) ex vivo. Soleus muscles from *pik3r1 mKO pik3r2*$^{-/-}$ mice showed

modestly impaired 2-deoxyglucose uptake in response to both submaximal (0.6mU/ml) and maximal (50mU/ml) doses of insulin (Figure 4A). EDL muscles were only responsive to maximal insulin, and 2-deoxyglucose uptake in EDL muscles from *pik3r1 mKO pik3r2*$^{-/-}$ mice was also impaired (Figure 4A). Thus the loss of muscle PI3K signaling in *pik3r1 mKO pik3r2*$^{-/-}$ mice led to muscle insulin resistance, although the effect was not as severe as might have been expected considering the dramatic reduction in muscle Akt signaling (Figure 1). Consistent with this, we found that *pik3r1 mKO pik3r2*$^{-/-}$ mice to have lower muscle glycogen content in the fed state compared to control animals (Figure 4B).

We investigated the possibility that muscle insulin resistance was sufficient to perturb whole-body glucose homeostasis in *pik3r1 mKO pik3r2*$^{-/-}$ mice. We first assessed whole-body glucose disposal using the glucose tolerance test (GTT). Following the injection of a bolus dose of glucose, the *pik3r1 mKO pik3r2*$^{-/-}$ mice showed both higher peak blood glucose levels (at 60 min) and more sustained elevation in blood glucose levels compared to control mice (Figure 4C), indicating these animals were glucose intolerant. Such glucose intolerance was also observed when animals were placed on a high-fat diet for 12 weeks (Figure 4C). Despite impaired glucose disposal, insulin release during GTT, as well as insulin sensitivity during insulin tolerance tests were normal in *pik3r1 mKO pik3r2*$^{-/-}$ mice (Figures 4D and 4E). These mice also had normal fasting and fed blood glucose and serum insulin levels (Table 1). In addition, high-fat diet did not make them more insulin resistant than control animals during ITT (data not shown). Taken together, these results suggest that although muscle insulin resistance alone is sufficient to cause glucose intolerance, it is insufficient to cause hyperglycemia, and other insulin responsive tissues could compensate for the defect in muscle insulin-sensitivity.

Interestingly, deletion of *pik3r1* alone in muscle did not result in a significant effect on glucose disposal (Figures 4C and 4E). This is in stark contrast to mice with germline deletion of *pik3r1* where a dramatic increase in insulin-dependent glucose disposal is observed (Fruman et al., 2000; Ueki et al., 2002b; Terauchi et al., 1999). These results indicate that tissues other than muscle are responsible for the enhanced insulin response in mice lacking p85α.

We next investigated whether adipose tissue, another major site of glucose disposal, might compensate for the reduction in muscle insulin resistance in *pik3r1 mKO pik3r2*$^{-/-}$ mice and thus maintain whole-body glucose homeostasis. A DEXA scan analysis of body fat content in age- and weight-matched animals revealed that *pik3r1 mKO pik3r2*$^{-/-}$ mice showed an approximately 30% increase in body fat (Figure 5A). Similarly, epididymal fat pads from these mice were approximately 70% heavier than those from control mice when adjusted to body weight (Figure 5B). The increased adiposity in *pik3r1 mKO pik3r2*$^{-/-}$ mice was accompanied by an increase in serum lipid levels. Fasting serum free fatty acids in *pik3r1 mKO pik3r2*$^{-/-}$ mice were approximately 30% higher than those from control mice, whereas fasting and fed serum triglycerides levels in these animals were over 60% higher than those from control animals (Figures 5C and 5D, Table 1). Taken together, these results suggest that muscle insulin resistance in *pik3r1 mKO pik3r2*$^{-/-}$ mice triggers compensatory metabolic changes that lead to increased adiposity and elevated circulating lipid levels, two symptoms that are also associated with human type 2 diabetes.

Discussion

The evolutionarily conserved PI3K signaling pathway is an important regulator of growth and metabolism. In the present study we have shown that the deletion of the p85α/p55α/p50α and p85β regulatory subunits of class I_A PI3K in the muscle severely impairs PI3K signaling and leads to decreased muscle size, decreased insulin-stimulated muscle glucose uptake, and impaired whole-body glucose disposal. These results demonstrate genetically that p85 is essential for class I_A PI3K signaling in vivo and muscle PI3K signaling critically regulates myocyte size and muscle metabolism. In addition, we found that loss of muscle PI3K signaling leads to indirect effects on the adipose tissue and causes increased adiposity and elevated levels of circulating lipids.

The p85 regulatory subunit of class I_A PI3K is essential for the stability of the p110 catalytic subunit and is required to mediate the receptor/adaptor recruitment and activation of p110 (Brachmann et al., 2005; Yu et al., 1998a, 1998b). Germline knockout mice lacking various p85 isoforms, however, all exhibited improved PI3K signaling (Chen et al., 2004; Terauchi et al., 1999; Ueki et al., 2002b; Mauvais-Jarvis et al., 2002). It was subsequently shown that in cells in culture, p85 is often stoichiometrically in excess of p110, and in its monomeric form p85 negatively regulate PI3K signaling (Ueki et al., 2002a, 2003). Monomeric p85 competes with the p85-p110 heterodimer for IRS binding and drives the formation of large, nonsignaling sequestration complexes with IRS-1 in the cytosol (Luo et al., 2005a). These in vitro studies offer a possible explanation for why a partial loss of p85 in vivo results in increased insulin sensitivity.

The attempt to understand the role of p85 in insulin signaling in vivo has been precluded by the perinatal lethality associated with mice with germline deletion of the *pik3r1* gene and the embryonic lethality associated with mice doubly null for the *pik3r1* and *pik3r2* genes (Brachmann et al., 2005; Fruman et al., 2000). In addition, the crosstalk between different insulin-responsive tissues in vivo makes it difficult to elucidate the tissue-specific roles of p85 and PI3K in the regulation of metabolism. To overcome these drawbacks, we have generated a conditional (floxed) *pik3r1* allele that allows tissue-specific deletion of this gene using the Cre-lox approach (Luo et al., 2005b).

When we crossed *pik3r1*$^{fl/fl}$ mice with *mck-cre* mice, we observed efficient deletion of p85α, p55α, and p50α, accompanied by a significant reduction in p110α level (Figure 1A). Consequently, muscle PI3K activation is severely impaired (Figure 1B). This provides direct evidence that p85 is essential for both the stability and activation of p110 in vivo. The severe impairment in muscle PI3K signaling in *pik3r1 mKO* mice, however, did not translate into severely impaired Akt signaling downstream (Figure 1C). This suggests that p85β was able to compensate for the loss of all p85α isoforms in the muscle. The discordance between the amount of PI3K bound to IRS proteins and the magnitude of Akt activation observed in the *pik3r1 mKO* mice versus *pik3r1 mKO pik3r2*$^{-/-}$ mice is consistent with the idea that only a small fraction of the PI3K bound to IRS-1 is utilized to generate the PIP_3 required for Akt activation, as argued in the IRS-1 sequestration model (Luo et al., 2005a). Consistent with the relatively normal activation of Akt in the *pik3r1 mKO* mice, myocyte size and muscle metabolism both appeared normal in these mice. The normal Akt activation in the muscle of *pik3r1 mKO* mice also mirrored that observed in muscle from

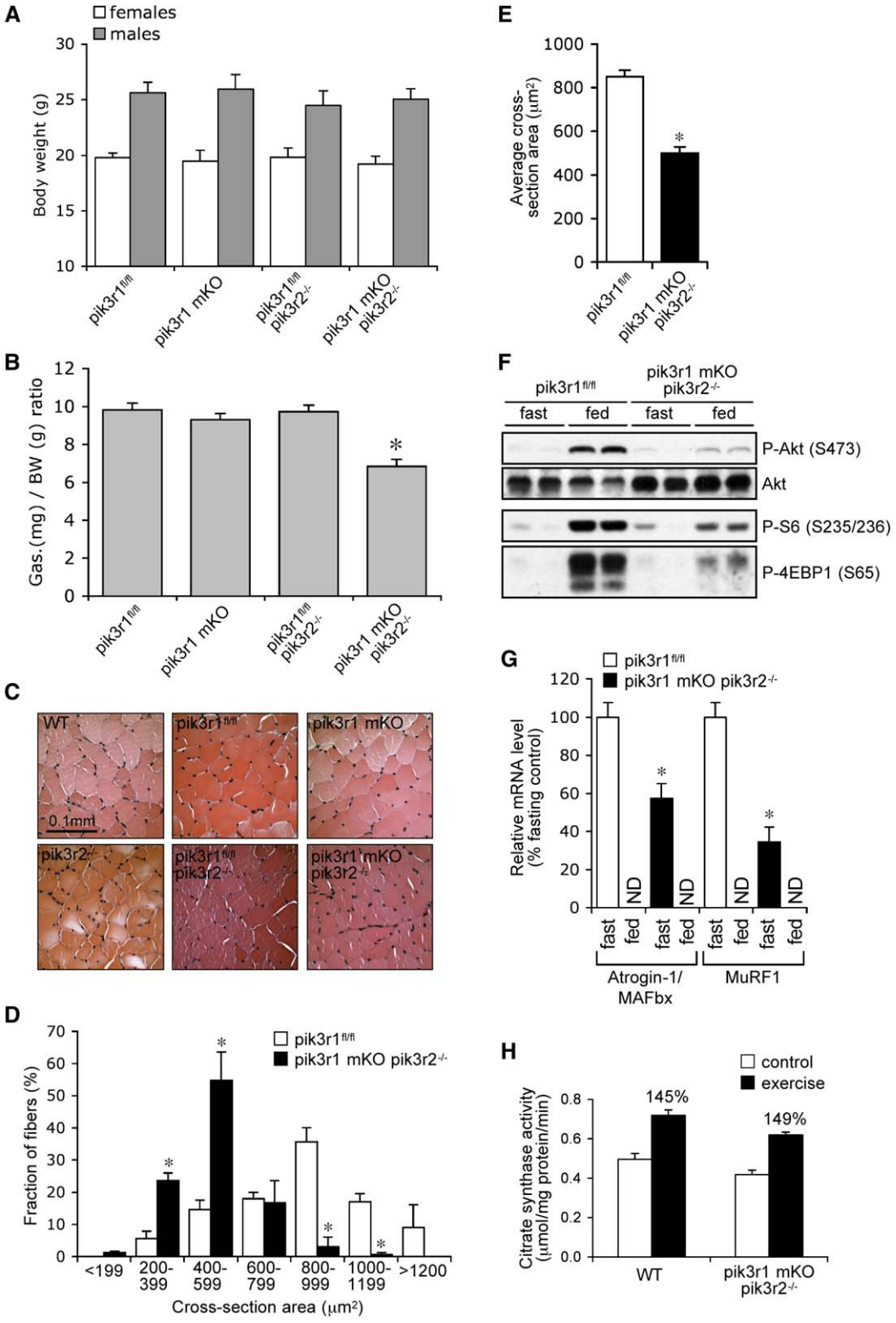

Figure 3. *pik3r1 mKO pik3r2*$^{-/-}$ mice have reduced muscle weight and myocyte size

A) Body weight of 8 week-old mice.

B) Gastrocnemius muscle to body weight ratio of age-matched male mice (n = 6, *p < 0.01 compared to *pik3r1*$^{fl/fl}$ mice). Similar results were obtained for female mice (data not shown).

C) Representative cross-section of tibialis anterior (TA) muscle with H&E stain.

D) Distribution of TA muscle myocyte cross-section area in age- and body-weight-matched control and *pik3r1 mKO pik3r2*$^{-/-}$ mice (n = 3, *p < 0.01 compared to the number of myocytes in the same size range in *pik3r1*$^{fl/fl}$ mice).

E) Mean TA muscle myocyte cross-section area as shown in (**D**) (n = 3, *p < 0.01 compared to *pik3r1*$^{fl/fl}$ mice).

the *pik3r1* germline knockout mice (Fruman et al., 2000). The *pik3r1 mKO* mice exhibited normal glucose tolerance during GTT and normal fasting and fed blood glucose levels. This indicates that the hypoglycemic and insulin hypersensitive phenotype of the germline *pik3r1* knockout mice cannot be attributed to the loss of *pik3r1* in the muscle (see below).

To achieve the complete ablation of all p85 regulatory subunits in the muscle, we further crossed *pik3r1 mKO* mice with *pik3r2*$^{-/-}$ mice. Both PI3K activation and Akt signaling were severely impaired in the muscles of *pik3r1 mKO pik3r2*$^{-/-}$ mice, resulting in growth and metabolic defects. Some residual amount of p85 proteins and class I_A PI3K activity remained in the muscles of *pik3r1 mKO pik3r2*$^{-/-}$ mice. This could be due to incomplete deletion of the *pik3r1* gene in a few myocytes, or contribution from nonmyocyte cells in the muscle such as satellite cells, endothelium and adipocytes. Dramatic upregulation of p55γ has been observed in *pik3r1*$^{-/-}$*pik3r2*$^{-/-}$ MEFs in compensation for the loss of all other p85 isoforms (Brachmann et al., 2005). We did not detect significant levels of p55γ proteins in muscles from either control or *pik3r1 mKO pik3r2*$^{-/-}$ mice (data not shown). Thus it is unlikely that p55γ is dramatically upregulated in the muscle of *pik3r1 mKO pik3r2*$^{-/-}$ mice, although our inability to detect p55γ in the muscle could also be attributed toward the lack of antibody sensitivity.

Genetic studies in mice indicate that the IGF-1/PI3K signaling pathway regulates growth and development. Germline deletion of the IGF-1 receptor results in severe growth retardation (Liu et al., 1993), whereas cardiac-specific expression of IGF-1 receptor results in enlarged hearts (McMullen et al., 2004). We have previously shown that *pik3r1 mKO pik3r2*$^{-/-}$ mice have reduced heart size (Luo et al., 2005b), whereas the cardiac overexpression of a constitutively active form of p110 increases heart size (Shioi et al., 2000). Genetic manipulation of PTEN and Akt also leads to development and growth phenotypes (Backman et al., 2001; Chen et al., 2001; Kwon et al., 2001; Cho et al., 2001b; Groszer et al., 2001). In the present study we show that the loss of PI3K signaling in the muscle results in reduced muscle weight and myocyte size (Figures 3B–3E), thus demonstrating a key role of PI3K in the regulation of muscle growth. Interestingly, class I_A PI3K appears to exclusively regulate muscle growth and fiber size, as fiber structure and the ability of the muscle to respond to increased exercise load appear minimally impacted by the loss of PI3K signaling (Figures 3C and 3H). It remained to be determined, however, whether loss of PI3K signaling also negatively impact muscle contractility.

The mTOR pathway that controls protein synthesis and cell growth is likely to contribute toward the small muscle phenotype observed in *pik3r1 mKO pik3r2*$^{-/-}$ mice (Rommel et al., 2001). Both insulin and IGF-1 stimulated tuberin phosphorylation by Akt in the muscle was impaired in these mice (Figures 1C and 2B). In addition, muscle Akt, S6 and 4EBP1 phosphorylation in response to feeding was also diminished in *pik3r1 mKO pik3r2*$^{-/-}$ mice (Figure 3F). Thus a reduction in protein synthesis could, at least in part, account for the reduction in muscle size. Protein degradation through forkhead-mediated expression of E3-ubiquitin ligases atrogin-1/MAFbx and MuRF1 have been implicated in the regulation of muscle atrophy (Sandri et al., 2004; Stitt et al., 2004). To our surprise, albeit still strongly induced by fasting, the muscle mRNA levels of atrogin-1/MAFbx and MuRF1 in fasting *pik3r1 mKO pik3r2*$^{-/-}$ mice were actually lower than that of control mice (Figure 3F). The mechanisms behind such attenuation are unclear, although there might be several potential explanations. It is possible that normally skeletal muscle serves as a source of amino acids during prolonged fast. In the *pik3r1 mKO pik3r2*$^{-/-}$ mice, however, the loss of PI3K signaling and reduction in muscle mass may trigger a negative feedback loop that attenuates muscle protein mobilization in the fasting state and prevents excessive muscle loss. In addition, the increased body fat content in the *pik3r1 mKO pik3r2*$^{-/-}$ mice, together with an elevation in serum lipid and fasting leptin levels (Figure 5 and Table 1) might also signal to prevent muscle protein breakdown.

Muscle insulin resistance is a major contributor to human type 2 diabetes (Shulman, 2004). Deletion of PTEN in the muscle leads to enhanced insulin sensitivity and protection from diet-induced insulin resistance (Wijesekara et al., 2005). Muscle insulin sensitivity and global glucose tolerance of *pik3r1 mKO* mice appeared normal (Figure 4 and data not shown), suggesting that the hypoglycemia and insulin hypersensitivity phenotype seen in the germline *pik3r1*$^{-/-}$ mice cannot be attributed to the muscle. In a parallel study, we and collaborators have observed that liver-specific *pik3r1* deletion recapitulates the improved insulin-dependent serum glucose regulation observed in germline *pik3r1* deletion (C. Taniguchi, J.L., L.C.C., C.R. Kahn, et al., submitted).

Muscles from *pik3r1 mKO pik3r2*$^{-/-}$ mice show reduced glucose transport in response to insulin, this in turn leads to reduced muscle glycogen content in the fed state and modest but significant glucose intolerance during GTT (Figure 3). Such glucose intolerance might also be partially attributable to the elevated body fat content in these mice. Nevertheless, these animals were able to maintain normal fasting and fed glucose and insulin levels (Table 1). This suggests muscle insulin resistance alone, at least in mice, is insufficient to cause diabetes. Our findings largely recapitulate the phenotypes of muscle-specific insulin receptor knockout (MIRKO) mice (Bruning et al., 1998; Kim et al., 2000). Thus in muscle PI3K is likely to mediate most (if not all) of the metabolic effect of insulin. Mice with muscle-specific GLUT4 deletion exhibit more severe perturbation in glucose homeostasis than both the *pik3r1 mKO pik3r2*$^{-/-}$ mice and the MIRKO mice (Zisman et al., 2000). This difference could, at least in part, be attributed to the loss of basal glucose transport in the muscle GLUT4 KO mice that was not observed in the latter two mouse models.

Interestingly, muscle insulin resistance in *pik3r1 mKO pik3r2*$^{-/-}$ mice leads to altered lipid metabolism, similar to that observed in the MIRKO mice. We observed elevated levels of circulating fatty acids and triglycerides in these animals that were associated with significantly increased body fat content (Figure 5). The increase in fat mass appeared to compensate

F) Gastrocnemius muscle lysates from fasting and fed mice were probed for Akt, S6 and 4EBP1 phosphorylation to examine feeding-induced activation of the Akt/mTOR pathway.
G) Muscle atrogin-1/MAFbx and MuRF1 mRNA levels in fasting mice as measured by real-time RT-PCR (n = 3, *p < 0.05 compared to *pik3r1*$^{fl/fl}$ mice; ND, not detectable).
H) Muscle citrate synthase activity in sedentary mice and mice that were subjected to swim exercise for 1 month. The percentage change in exercise-induced elevation from basal level of the same genotype was also shown (n = 6). All error bars represent standard errors of the mean.

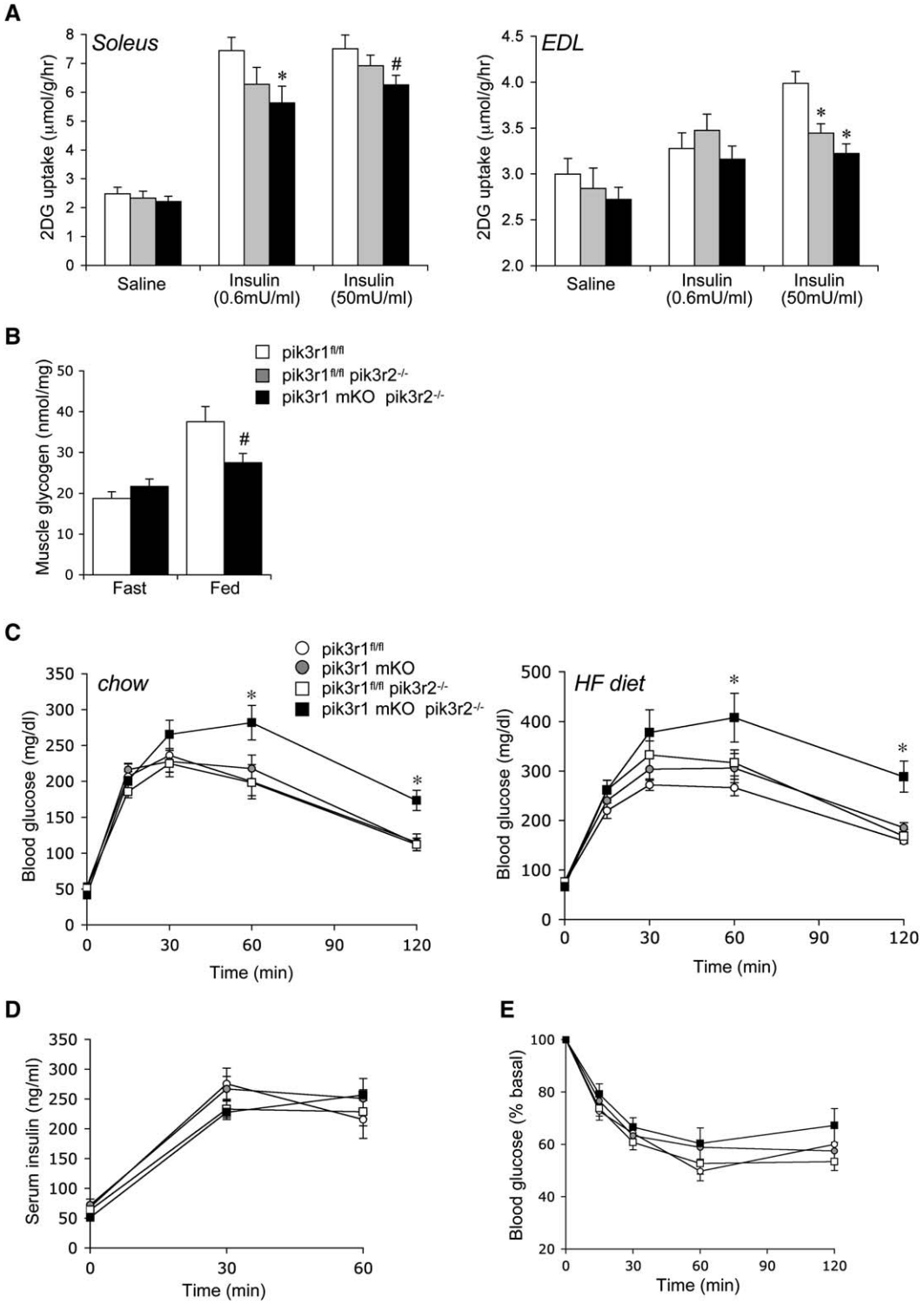

Figure 4. *pik3r1 mKO pik3r2*$^{-/-}$ mice exhibit muscle insulin resistance and glucose intolerance

A) Insulin-stimulated 2-deoxyglucose (2DG) uptake in isolated soleus and EDL muscle (n = 5–6, #p < 0.06 and *p < 0.01 compared to *pik3r1*$^{fl/fl}$ mice of the same treatment group).

B) Muscle glycogen content in fast and fed mice (n = 3, #p< 0.08 compared to *pik3r1*$^{fl/fl}$ animals of the same group).

C) Glucose tolerance test of 5-month-old males on regular-chow or high-fat (HF) diet (n = 6–8, *p < 0.05 compared to *pik3r1*$^{fl/fl}$ mice at the same time point).

D) Serum insulin level of 5-month-old males on regular chow diet during DTT as shown in **C** (n = 6).

E) Insulin tolerance test of 5-month-old males on regular chow diet (n = 6–8). All error bars represent standard errors of the mean.

Table 1. Metabolic parameters of mice in this study

	Glucose (mg/dL)		Insulin (ng/ml)		Leptin (ng/ml)		FFAs (mEq/L)		TG (mg/ml)	
Genotype	fast	fed	fast	fed	fast	fed	fast	fed	fast	fed
pik3r1$^{fl/fl}$	53 ± 5	122 ± 6	0.38 ± 0.06	1.28 ± 0.23	2.2 ± 0.7	12.5 ± 1.4	1.24 ± 0.09	1.10 ± 0.10	2.32 ± 0.48	3.10 ± 0.39
pik3r1 mKO	49 ± 2	124 ± 11	0.23 ± 0.03	1.19 ± 0.21	2.9 ± 1.1	11.9 ± 2.2	1.67 ± 0.24	0.86 ± 0.14	3.60 ± 0.79	3.70 ± 0.44
pik3r1$^{fl/fl}$ *pik3r2*$^{-/-}$	51 ± 3	135 ± 9	0.35 ± 0.04	0.98 ± 0.20	1.4 ± 0.7	9.4 ± 1.6	1.36 ± 0.04	0.97 ± 0.15	2.81 ± 0.27	3.49 ± 0.64
pik3r1 mKO pik3r2$^{-/-}$	41 ± 2	135 ± 7	0.45 ± 0.09	1.20 ± 0.22	5.0 ± 1.0*	13.8 ± 2.7	1.63 ± 0.15*	1.02 ± 0.10	3.73 ± 0.55	5.22 ± 0.59*

n = 6–8, *p < 0.05 compared to *pik3r1*$^{fl/fl}$ mice of the same group, errors represent standard errors of the mean. FFAs, free fatty acids; TG, triglycerides.

for the reduction in muscle mass in *pik3r1 mKO pik3r2*$^{-/-}$ mice, thus we did not observe an overall change in body weight. This metabolic shift could be explained by the conversion of glucose to lipids in these animals: the reduced muscle glucose disposal causes elevated lipid synthesis by the liver and increased glucose uptake in adipocytes, thus leading to increased fat storage (Kim et al., 2000). These findings highlight the crosstalk between different insulin-responsive tissues in vivo in the coordinated regulation of glucose homeostasis. The hyperlipidemia and adiposity phenotype of *pik3r1 mKO pik3r2*$^{-/-}$ mice resembles similar symptoms associated with human type 2 diabetes, indicating muscle insulin resistance is at least partially responsible for the perturbation in lipid metabolism in type 2 diabetes.

Germline knockout mice lacking the insulin receptor exhibit mild growth retardation but severe metabolic defects (Accili et al., 1996; Joshi et al., 1996). In contrast, mice lacking the IGF-1 receptor exhibit severe growth retardation (Liu et al., 1993). These and other studies indicate that in mammals insulin primarily regulates metabolism where as IGF-1 primarily regulates growth and development. A parallel has been drawn with Akt1 and Akt2: Akt1 KO mice show growth retardation without significant alterations in insulin sensitivity (Chen et al., 2001; Cho et al., 2001b), whereas mice lacking Akt2 show glucose intolerance and insulin resistance (Cho et al., 2001a). The phenotypes of the *pik3r1 mKO pik3r2*$^{-/-}$ mice recapitulate both that of the insulin and IGF-1 KO mice and that of the Akt1 and Akt2 KO mice. Thus in the muscle of these mice both Akt1 and Akt2 activation are severely impaired in response to either insulin or IGF-1 stimulation. As a result, the muscle of these animals is both small and insulin resistant. Our findings therefore indicate that in the muscle class I_A PI3K is a critical activator of both Akt1 and Akt2 downstream of insulin and IGF-1 signaling. This raises the question of how insulin and IGF-1, as well as Akt1 and Akt2, regulate different aspects of muscle physiology while

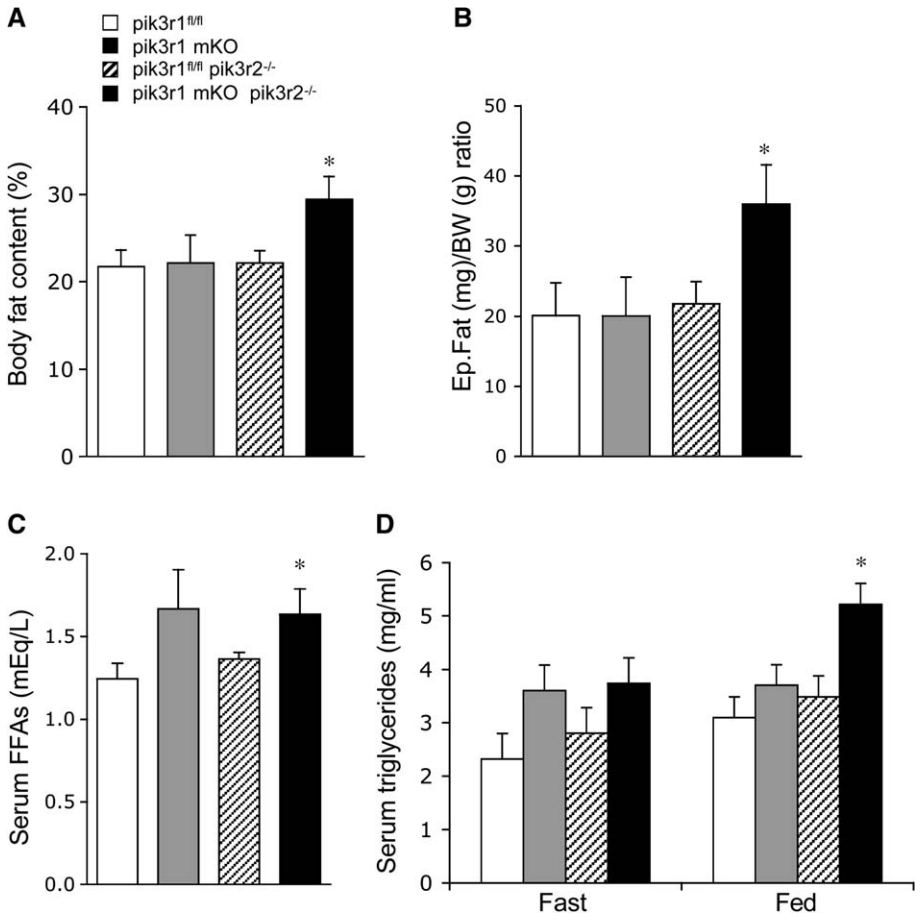

Figure 5. *pik3r1 mKO pik3r2*$^{-/-}$ mice have increase body fat content and elevated circulating lipid levels

A) Body fat content as measured by DEXA scan in 5-month old males on regular chow diet (n = 6, *p < 0.05 compared to *pik3r1*$^{fl/fl}$ mice).

B) Epididymal fat pad to body weight ratio in 5-month-old males on regular chow diet (n = 6, *p < 0.05 compared to *pik3r1*$^{fl/fl}$ mice).

C) Fasting serum free fatty acids (FFAs) levels in 5-month-old males on regular chow diet (n = 6, *p < 0.05 compared to *pik3r1*$^{fl/fl}$ mice of the same group).

D) Fasting and fed serum triglycerides levels in 5-month-old males on regular chow diet (n = 6, *p < 0.05 compared to *pik3r1*$^{fl/fl}$ mice of the same group). All error bars represent standard errors of the mean.

utilizing class I_A PI3Ks as a common signaling node (Taniguchi et al., 2006). It is possible that under physiological conditions, insulin and IGF-1 might elicit different magnitude and duration of PI3K signaling that preferentially activate different downstream targets (e.g., Akt1 vs. Akt2). In addition, insulin and IGF-1 receptors might also differentially activate other signaling pathways that corroborate with PI3K-Akt to determine signaling outcome.

In conclusion, our current work demonstrate that class I_A PI3K signaling is a critical regulator of both muscle size and muscle insulin sensitivity in vivo. These findings have broad implication in the understanding of growth and metabolic regulation. In addition, our study indicates that attenuated muscle PI3K signaling could be an important pathological mechanism that underlies type 2 diabetes.

Experimental procedures

The *pik3r1*$^{fl/fl}$ mice, *pik3r2*$^{-/-}$ and *mck-cre* mice have all been described previously (Bruning et al., 1998; Ueki et al., 2002b; Luo et al., 2005b). All mice were maintained on a 129Sv-C57BL/6-FVB mixed background. Animal care and experimentations were approved by the Institutional Animal Care and Use Committees of Beth Israel Deaconess Medical Center and Harvard Medical School.

Glucose tolerance test (GTT) and insulin tolerance test (ITT) were performed as described previously (Ueki et al., 2002b). For GTT, mice were fasted overnight prior to intraperitoneal injection with glucose solution (2 mg/kg). For ITT mice were fasted for 4 hr prior to intraperitoneal injection with insulin solution (1 U/kg). Blood glucose was monitored using a glucometer (Bayer). For high-fat diet treatment, mice were place on a fat-adjusted diet (50% calories from fat) for 12 weeks. For aerobic exercise training, mice were subjected to 2 sessions of 90 min swim training daily for 1 month as described previously (McMullen et al., 2003).

Isolated muscle glucose transport was assayed as described previously (Bruning et al., 1998). In brief, isolated soleus or EDL muscles from mice that were fasted overnight were preincubated in gassed (95% O_2, 5% CO_2) Krebs-Ringer-Bicarbonate (KRB) buffer (117 mM NaCl, 4.7 mM KCl, 2.5 mM $CaCl_2$, 1.2 mM KH_2PO_4, 1.2mM $MgSO_4$, 24.6 mM $NaHCO_3$) with 2 mM pyruvate containing 0, 0.6 mU/ml or 50 mU/ml insulin at 30ºC for 40 min. Transport was measured in KRB containing 1mM 2-deoxy-D-[1,2-^{3}H]-glucose and 7mM D-[^{14}C]-mannitol at 37ºC for 10 min. Muscle glycogen level was measured as described previously (Musi et al., 2005).

Whole-body fat content measurement was carried out in anesthetized mice using a DEXA-scan X-ray imaging station according to the manufacturer's instructions (GE healthcare). Myocyte cross-section area was quantified using Image-J software (N.I.H.). At least 100 myocytes were measure per animal. Serum insulin and leptin levels were measured by ELISA according to manufacturer's instructions (Crystal Chem Inc.). Serum free fatty acids and triglycerides were measured by enzymatic reactions according to manufacturer's instructions (Sigma Aldrich). Muscle citrate synthase activity was measured by enzymatic method as described previously (McMullen et al., 2003).

Insulin stimulation in vivo and muscle lysate preparation was carried out as described previously (Taniguchi et al., 2005; Ueki et al., 2002b). In brief, mice were fasted overnight and deep anesthetized. Insulin (5 U/kg) was injected through the inferior vena cava, 5 min later the animals were sacrificed and muscle samples were collected. IGF-1 injection (1mg/kg) was performed similarly and muscle samples were collected 7 min following injection. Muscle lysates were prepared by homogenizing muscle samples in lysis buffer (25 mM Tris-HCl [pH 7.4], 10 mM EDTA, 10 mM EGTA, 100 mM NaF, 50 mM NaPPi, 1% NP-40, 10 mM Na3VO4, 1 mM dithiothreitol, 2 mM phenylmethylsulfonyl fluoride, 8 g/ml leupeptin, 8 g/ml aprotinin, and 8 g/ml pepstatin) followed by centrifugation at 150,000 × g for 20 min.

Antibody against p85 (which reacts strongly with p85α and weakly with p85β), antibody against phosphotyrosine (4G10) and antibodies against IRS-1 and IRS-2 were described previously (Ueki et al., 2002b; Fruman et al., 2000). Antibody against p110α was from BD Biosciences. Antibody against the insulin receptor β-subunit, antibody against the IGF-1 receptor β-subunit, and antibody against tuberin were from Santa Cruz Technologies. Antibody against α-tubulin was from Sigma. All other antibodies were from Cell Signaling Technology.

The in vitro PI3K assay was carried out as described previously (Fruman et al., 2000). Briefly, IRS-1 or IRS-2 immunoprecipitates from muscle lysates was incubated with phosphatidylinositol (Avanti) and γ-^{32}P-ATP in kinase buffer containing 20 mM Tris-HCl (pH 7.4), 100 mM NaCl, and 0.5 mM EGTA. The lipid product was extracted in chloroform, separated by thin-layer chromatography and quantified using a phosphorimager screen (Amersham Biosciences).

For real-time RT-PCR quantification of muscle atrogin-1/MAFbx and MuRF1 mRNA levels, mice were fasted for 36 hr (fast) and fed for 8 hr (fed). Muscle total RNA was extracted using the RNeasy kit (Qiagen). The following primers were used for RT-PCR: atrogin-1/MAFbx forward 5′-CTC TGT ACC ATG CCG TTC CT-3′, reverse 5′-GGC TGC TGA ACA GAT TCT CC-3′; MuRF1 forward 5′-ACG AGA AGA AGA GCG AGC TG-3′, reverse 5′-CTT GGC ACT TGA GAG GAA GG-3′; GAPDH forward 5′-CGT CCC GTA GAC AAA ATG GT-3′, reverse 5′-GAA TTT GCC GTG AGT GGA GT-3′. Real-time RT-PCR was carried using the SYBR green method (Applied Biosystems). Atrogin-1/MAFbx and MuRF1 mRNA levels were normalized against GAPDH mRNA.

Statistical analysis was carried out using Prism 4 (Graphpad Software) and Microsoft Excel Statistics Toolkit (Microsoft). ANOVA and Student's t tests were applied. Results shown are mean±SEM, a p-value of <0.05 was considered to be statistically significant.

Acknowledgments

We thank S. White and D. Brown for assistance with tissue histology. We thank C.M. Taniguchi, C.R. Kahn, K.A. Lamia, S.M. Brachmann, A.L. Goldberg, J. Blenis, J. Yuan, and T. Roberts for advice. This work is supported by a Howard Hughes Predoctoral Fellowship to J.L., by NIH grants AR42238 and DK 068626 to L.J.G., and by NIH grants GM41890 and CA089021 to L.C.C.

Received: December 15, 2005
Revised: March 12, 2006
Accepted: April 13, 2006
Published: May 9, 2006

References

Accili, D., Drago, J., Lee, E.J., Johnson, M.D., Cool, M.H., Salvatore, P., Asico, L.D., Jose, P.A., Taylor, S.I., and Westphal, H. (1996). Early neonatal death in mice homozygous for a null allele of the insulin receptor gene. Nat. Genet. *12*, 106–109.

Backman, S.A., Stambolic, V., Suzuki, A., Haight, J., Elia, A., Pretorius, J., Tsao, M.S., Shannon, P., Bolon, B., Ivy, G.O., and Mak, T.W. (2001). Deletion of Pten in mouse brain causes seizures, ataxia and defects in soma size resembling Lhermitte-Duclos disease. Nat. Genet. *29*, 396–403.

Barthel, A., Schmoll, D., and Unterman, T.G. (2005). FoxO proteins in insulin action and metabolism. Trends Endocrinol. Metab. *16*, 183–189.

Bayascas, J.R., and Alessi, D.R. (2005). Regulation of Akt/PKB Ser473 phosphorylation. Mol. Cell *18*, 143–145.

Bodine, S.C., Stitt, T.N., Gonzalez, M., Kline, W.O., Stover, G.L., Bauerlein, R., Zlotchenko, E., Scrimgeour, A., Lawrence, J.C., Glass, D.J., and Yancopoulos, G.D. (2001). Akt/mTOR pathway is a crucial regulator of skeletal muscle hypertrophy and can prevent muscle atrophy in vivo. Nat. Cell Biol. *3*, 1014–1019.

Brachmann, S.M., Yballe, C.M., Innocenti, M., Deane, J.A., Fruman, D.A., Thomas, S.M., and Cantley, L.C. (2005). Role of phosphoinositide 3-kinase regulatory isoforms in development and actin rearrangement. Mol. Cell. Biol. *25*, 2593–2606.

Bruning, J.C., Michael, M.D., Winnay, J.N., Hayashi, T., Horsch, D., Accili, D., Goodyear, L.J., and Kahn, C.R. (1998). A muscle-specific insulin receptor knockout exhibits features of the metabolic syndrome of NIDDM without altering glucose tolerance. Mol. Cell *2*, 559–569.

Burgering, B.M., and Medema, R.H. (2003). Decisions on life and death: FOXO Forkhead transcription factors are in command when PKB/Akt is off duty. J. Leukoc. Biol. *73*, 689–701.

Cantley, L.C. (2002). The phosphoinositide 3-kinase pathway. Science *296*, 1655–1657.

Chen, D., Mauvais-Jarvis, F., Bluher, M., Fisher, S.J., Jozsi, A., Goodyear, L.J., Ueki, K., and Kahn, C.R. (2004). p50alpha/p55alpha phosphoinositide 3-kinase knockout mice exhibit enhanced insulin sensitivity. Mol. Cell. Biol. *24*, 320–329.

Chen, W.S., Xu, P.Z., Gottlob, K., Chen, M.L., Sokol, K., Shiyanova, T., Roninson, I., Weng, W., Suzuki, R., Tobe, K., et al. (2001). Growth retardation and increased apoptosis in mice with homozygous disruption of the Akt1 gene. Genes Dev. *15*, 2203–2208.

Cho, H., Mu, J., Kim, J.K., Thorvaldsen, J.L., Chu, Q., Crenshaw, E.B., 3rd, Kaestner, K.H., Bartolomei, M.S., Shulman, G.I., and Birnbaum, M.J. (2001a). Insulin resistance and a diabetes mellitus-like syndrome in mice lacking the protein kinase Akt2 (PKB beta). Science *292*, 1728–1731.

Cho, H., Thorvaldsen, J.L., Chu, Q., Feng, F., and Birnbaum, M.J. (2001b). Akt1/PKBalpha is required for normal growth but dispensable for maintenance of glucose homeostasis in mice. J. Biol. Chem. *276*, 38349–38352.

Cohen, P., and Frame, S. (2001). The renaissance of GSK3. Nat. Rev. Mol. Cell Biol. *2*, 769–776.

Fruman, D.A., Mauvais-Jarvis, F., Pollard, D.A., Yballe, C.M., Brazil, D., Bronson, R.T., Kahn, C.R., and Cantley, L.C. (2000). Hypoglycaemia, liver necrosis and perinatal death in mice lacking all isoforms of phosphoinositide 3-kinase p85 alpha. Nat. Genet. *26*, 379–382.

Fruman, D.A., Meyers, R.E., and Cantley, L.C. (1998). Phosphoinositide kinases. Annu. Rev. Biochem. *67*, 481–507.

Groszer, M., Erickson, R., Scripture-Adams, D.D., Lesche, R., Trumpp, A., Zack, J.A., Kornblum, H.I., Liu, X., and Wu, H. (2001). Negative regulation of neural stem/progenitor cell proliferation by the Pten tumor suppressor gene in vivo. Science *294*, 2186–2189.

Guarente, L., and Kenyon, C. (2000). Genetic pathways that regulate ageing in model organisms. Nature *408*, 255–262.

Joshi, R.L., Lamothe, B., Cordonnier, N., Mesbah, K., Monthioux, E., Jami, J., and Bucchini, D. (1996). Targeted disruption of the insulin receptor gene in the mouse results in neonatal lethality. EMBO J. *15*, 1542–1547.

Kim, J.K., Michael, M.D., Previs, S.F., Peroni, O.D., Mauvais-Jarvis, F., Neschen, S., Kahn, B.B., Kahn, C.R., and Shulman, G.I. (2000). Redistribution of substrates to adipose tissue promotes obesity in mice with selective insulin resistance in muscle. J. Clin. Invest. *105*, 1791–1797.

Kwon, C.H., Zhu, X., Zhang, J., Knoop, L.L., Tharp, R., Smeyne, R.J., Eberhart, C.G., Burger, P.C., and Baker, S.J. (2001). Pten regulates neuronal soma size: a mouse model of Lhermitte-Duclos disease. Nat. Genet. *29*, 404–411.

Lai, K.M., Gonzalez, M., Poueymirou, W.T., Kline, W.O., Na, E., Zlotchenko, E., Stitt, T.N., Economides, A.N., Yancopoulos, G.D., and Glass, D.J. (2004). Conditional activation of akt in adult skeletal muscle induces rapid hypertrophy. Mol. Cell. Biol. *24*, 9295–9304.

LeRoith, D., Werner, H., Neuenschwander, S., Kalebic, T., and Helman, L.J. (1995). The role of the insulin-like growth factor-I receptor in cancer. Ann. N Y Acad. Sci. *766*, 402–408.

Liu, J.P., Baker, J., Perkins, A.S., Robertson, E.J., and Efstratiadis, A. (1993). Mice carrying null mutations of the genes encoding insulin-like growth factor I (Igf-1) and type 1 IGF receptor (Igf1r). Cell *75*, 59–72.

Luo, J., McMullen, J.R., Sobkiw, C.L., Zhang, L., Dorfman, A.L., Sherwood, M.C., Logsdon, M.N., Horner, J.W., Depinho, R.A., Izumo, S., and Cantley, L.C. (2005b). Class IA Phosphoinositide 3-Kinase Regulates Heart Size and Physiological Cardiac Hypertrophy. Mol. Cell. Biol. *25*, 9491–9502.

Luo, J., Field, S.J., Lee, J.Y., Engelman, J.A., and Cantley, L.C. (2005a). The p85 regulatory subunit of phosphoinositide 3-kinase down-regulates IRS-1 signaling via the formation of a sequestration complex. J. Cell Biol. *170*, 455–464.

Mauvais-Jarvis, F., Ueki, K., Fruman, D.A., Hirshman, M.F., Sakamoto, K., Goodyear, L.J., Iannacone, M., Accili, D., Cantley, L.C., and Kahn, C.R. (2002). Reduced expression of the murine p85alpha subunit of phosphoinositide 3-kinase improves insulin signaling and ameliorates diabetes. J. Clin. Invest. *109*, 141–149.

McMullen, J.R., Shioi, T., Huang, W.Y., Zhang, L., Tarnavski, O., Bisping, E., Schinke, M., Kong, S., Sherwood, M.C., Brown, J., et al. (2004). The insulin-like growth factor 1 receptor induces physiological heart growth via the phosphoinositide 3-kinase(p110alpha) pathway. J. Biol. Chem. *279*, 4782–4793.

McMullen, J.R., Shioi, T., Zhang, L., Tarnavski, O., Sherwood, M.C., Kang, P.M., and Izumo, S. (2003). Phosphoinositide 3-kinase(p110alpha) plays a critical role for the induction of physiological, but not pathological, cardiac hypertrophy. Proc. Natl. Acad. Sci. USA *100*, 12355–12360.

Mora, A., Komander, D., van Aalten, D.M., and Alessi, D.R. (2004). PDK1, the master regulator of AGC kinase signal transduction. Semin. Cell Dev. Biol. *15*, 161–170.

Musi, N., Hirshman, M.F., Arad, M., Xing, Y., Fujii, N., Pomerleau, J., Ahmad, F., Berul, C.I., Seidman, J.G., Tian, R., and Goodyear, L.J. (2005). Functional role of AMP-activated protein kinase in the heart during exercise. FEBS Lett. *579*, 2045–2050.

Richardson, C.J., Schalm, S.S., and Blenis, J. (2004). PI3-kinase and TOR: PIKTORing cell growth. Semin. Cell Dev. Biol. *15*, 147–159.

Rommel, C., Bodine, S.C., Clarke, B.A., Rossman, R., Nunez, L., Stitt, T.N., Yancopoulos, G.D., and Glass, D.J. (2001). Mediation of IGF-1-induced skeletal myotube hypertrophy by PI(3)K/Akt/mTOR and PI(3)K/Akt/GSK3 pathways. Nat. Cell Biol. *3*, 1009–1013.

Saltiel, A.R., and Kahn, C.R. (2001). Insulin signalling and the regulation of glucose and lipid metabolism. Nature *414*, 799–806.

Sandri, M., Sandri, C., Gilbert, A., Skurk, C., Calabria, E., Picard, A., Walsh, K., Schiaffino, S., Lecker, S.H., and Goldberg, A.L. (2004). Foxo transcription factors induce the atrophy-related ubiquitin ligase atrogin-1 and cause skeletal muscle atrophy. Cell *117*, 399–412.

Shioi, T., Kang, P.M., Douglas, P.S., Hampe, J., Yballe, C.M., Lawitts, J., Cantley, L.C., and Izumo, S. (2000). The conserved phosphoinositide 3-kinase pathway determines heart size in mice. EMBO J. *19*, 2537–2548.

Shulman, G.I. (2004). Unraveling the cellular mechanism of insulin resistance in humans: new insights from magnetic resonance spectroscopy. Physiology (Bethesda) *19*, 183–190.

Stitt, T.N., Drujan, D., Clarke, B.A., Panaro, F., Timofeyva, Y., Kline, W.O., Gonzalez, M., Yancopoulos, G.D., and Glass, D.J. (2004). The IGF-1/PI3K/Akt pathway prevents expression of muscle atrophy-induced ubiquitin ligases by inhibiting FOXO transcription factors. Mol. Cell *14*, 395–403.

Taniguchi, C.M., Emanuelli, B., and Kahn, C.R. (2006). Critical nodes in signalling pathways: insights into insulin action. Nat. Rev. Mol. Cell Biol. *7*, 85–96.

Taniguchi, C.M., Ueki, K., and Kahn, R. (2005). Complementary roles of IRS-1 and IRS-2 in the hepatic regulation of metabolism. J. Clin. Invest. *115*, 718–727.

Terauchi, Y., Tsuji, Y., Satoh, S., Minoura, H., Murakami, K., Okuno, A., Inukai, K., Asano, T., Kaburagi, Y., Ueki, K., et al. (1999). Increased insulin sensitivity and hypoglycaemia in mice lacking the p85 alpha subunit of phosphoinositide 3-kinase. Nat. Genet. *21*, 230–235.

Thong, F.S., Dugani, C.B., and Klip, A. (2005). Turning signals on and off: GLUT4 traffic in the insulin-signaling highway. Physiology (Bethesda) *20*, 271–284.

Tschopp, O., Yang, Z.Z., Brodbeck, D., Dummler, B.A., Hemmings-Mieszczak, M., Watanabe, T., Michaelis, T., Frahm, J., and Hemmings, B.A. (2005). Essential role of protein kinase B gamma (PKB gamma/Akt3) in postnatal brain development but not in glucose homeostasis. Development *132*, 2943–2954.

Ueki, K., Fruman, D.A., Brachmann, S.M., Tseng, Y.H., Cantley, L.C., and Kahn, C.R. (2002a). Molecular balance between the regulatory and catalytic subunits of phosphoinositide 3-kinase regulates cell signaling and survival. Mol. Cell. Biol. *22*, 965–977.

Ueki, K., Fruman, D.A., Yballe, C.M., Fasshauer, M., Klein, J., Asano, T., Cantley, L.C., and Kahn, C.R. (2003). Positive and negative roles of p85 alpha and p85 beta regulatory subunits of phosphoinositide 3-kinase in insulin signaling. J. Biol. Chem. *278*, 48453–48466.

Ueki, K., Yballe, C.M., Brachmann, S.M., Vicent, D., Watt, J.M., Kahn, C.R., and Cantley, L.C. (2002b). Increased insulin sensitivity in mice lacking p85beta subunit of phosphoinositide 3-kinase. Proc. Natl. Acad. Sci. USA *99*, 419–424.

Virkamaki, A., Ueki, K., and Kahn, C.R. (1999). Protein-protein interaction in insulin signaling and the molecular mechanisms of insulin resistance. J. Clin. Invest. *103*, 931–943.

Wijesekara, N., Konrad, D., Eweida, M., Jefferies, C., Liadis, N., Giacca, A., Crackower, M., Suzuki, A., Mak, T.W., Kahn, C.R., et al. (2005). Muscle-specific Pten deletion protects against insulin resistance and diabetes. Mol. Cell. Biol. *25*, 1135–1145.

Yu, J., Wjasow, C., and Backer, J.M. (1998a). Regulation of the p85/p110-alpha phosphatidylinositol 3′-kinase. Distinct roles for the n-terminal and c-terminal SH2 domains. J. Biol. Chem. *273*, 30199–30203.

Yu, J., Zhang, Y., McIlroy, J., Rordorf-Nikolic, T., Orr, G.A., and Backer, J.M. (1998b). Regulation of the p85/p110 phosphatidylinositol 3′-kinase: stabilization and inhibition of the p110alpha catalytic subunit by the p85 regulatory subunit. Mol. Cell. Biol. *18*, 1379–1387.

Zisman, A., Peroni, O.D., Abel, E.D., Michael, M.D., Mauvais-Jarvis, F., Lowell, B.B., Wojtaszewski, J.F., Hirshman, M.F., Virkamaki, A., Goodyear, L.J., et al. (2000). Targeted disruption of the glucose transporter 4 selectively in muscle causes insulin resistance and glucose intolerance. Nat. Med. *6*, 924–928.